Soft mode and energy gap in spin-wave spectrum in a second-order orientational phase transition. AFMR in $YFeO_3$

A. M. Balbashov, A. G. Berezin, Yu. M. Gufan, G. S. Kolyadko, P. Yu. Marchukov, and E. G. Rudashevskiĭ

Institute of General Physics, USSR Academy of Sciences
(Submitted 9 December 1986)
Zh. Eksp. Teor. Fiz. **93**, 302–315 (July 1987)

An appreciable energy gap of non-magnetoelastic origin was observed experimentally in the spectrum of the low-frequency (quasiferromagnetic) antiferromagnetic-resonance branch during a second-order spin-flip transition in a magnetic field directed along the **a** axis of the rhombic weak ferromagnet $YFeO_3$. A theory that takes into account the susceptibility in the antiferromagnetism-axis and the dissipation processes is developed. It follows from this theory that a relaxation mode of oscillations, which is "soft" in the transition in question, should exist besides the usual oscillatory AFMR modes. The energy gaps, the kinetic coefficients, the Dzyaloshinskiĭ field, and the ratio of the longitudinal and transverse susceptibilities are determined from an analysis of experimental data obtained in fields up to 130 kOe and at frequencies 60–400 GHz at room temperature.

INTRODUCTION

The dynamics of multisublattice magnets is usually described using equations of first order in the time derivatives of generalized coordinates. Among the equations of this type are the most widely used Landau-Lifshitz equations.[1] In a system of dynamic equations, the secular equation that describes the dependence of the natural frequencies ω_i of the magnetic subsystem on the external conditions and on the phenomenological parameters, takes in the general case (with allowance for damping) the form

$$\omega^{3n}+\omega^{3n-1}\mathrm{Sp}_1R+\omega^{3n-2}\mathrm{Sp}_2R+\ldots\omega\mathrm{Sp}_{3n-1}R+\Delta_1\Delta_2=0. \quad (1)$$

Here Sp_iR are the traces of derivative matrices constructed in a definite manner from the dynamic matrix R (Ref. 2); n is the number of magnetic sublattices; $\Delta_1\Delta_2$ is the determinant of the dynamic matrix R, and is a product of the determinant Δ_1 of the matrix of the kinetic coefficients (in the Landau-Lifshitz equations these are the g-factors and the relaxation parameters) and the determinant Δ_2 of the system-stability matrix (discriminant matrix) whose elements are the derivatives of the Landau potential with respect to the components of the generalized coordinates that describe the dynamics of the systems (the projections of the sublattice magnetic-moment sublattices for one method of description or spin densities in the symmetry approach). In some papers (e.g., Ref. 3) account is taken also of inertia, and then the equations that describe the system dynamics contain second derivatives with respect to time.[4] In the general case, analysis of the magnetic-subsystem Lagrangian which depends on the generalized coordinates and velocities[5,6] leads to a secular equation of the form

$$\omega^{6n}+\omega^{6n-1}\mathrm{Sp}_1R+\ldots+\omega\mathrm{Sp}_{6n-1}R+\Delta_1\Delta_2=0 \quad (2)$$

(the notation is the same as above).

It can be seen that in all the dynamic descriptions the free term of the secular equation is proportional to the determinant of the stability matrix. As a result, one of the roots of the secular equation always vanishes on the stability-loss lines. In particular, in second-order phase transitions, when the stability-loss line of some phase coincides with the transition line, at least one of the roots of the secular equation goes through zero. A real root is said to correspond to a soft mode in the active subsystem,[7–9] and an imaginary root to a soft relaxator.[10] This general property of dynamic systems is preserved if the dynamics equations have a special form (e.g., the Landau-Lifshitz equations, where the determinant Δ_1 of the kinetic coefficients is identically zero). The vanishing of Δ_1 means simply that several integrals of the motion exist. In the Landau-Lifshitz equations these integrals are the squares of the sublattice magnetic moments. It is necessary in this case to exclude right away from consideration the cyclic coordinates and the form (1) of the secular equation, where everything pertains to noncyclic generalized coordinates is preserved, but the degree of the equation is lowered. Note that neglect of dissipation also causes Δ_1 to vanish; in this case the integral of the motion is the total energy of the magnetic subsystem.

Thus, it can be stated rigorously that on the stability-loss lines one of the natural frequencies (of the reciprocal relaxation times) always goes through zero. In a phenomenological description of the dynamics of magnets, however, a situation is possible in which the use of equations of motion of special form presupposes the existence of several integrals of the motion, which in fact they are not. In this case, a number of natural frequencies of the magnetic subsystem drop out, including possibly also those which should vanish in a phase transition.

Our aim here is to call attention to cases in which a soft mode is not the long-lived spin-wave excitation that is studied, in particular, in experiments on antiferromagnetic resonance. All the frequencies of the usual AFMR modes can in this case differ from zero at the second-order phase-transition point even if there is no interaction between the magnetic and elastic subsystems.

Note that gaps of nonmagnetoelastic origin were apparently already observed earlier in the AFMR spectra for spin-flip phase transitions. For example, it follows from data on AFMR in $YCrO_3$ (Ref. 11) that a gap reaching 40–60 GHz exists in a field in which spin flip takes place, whereas the magnetoelastic gap, according to our estimates, amounts to only[1)] 15–20 GHz.

 0038-5646/87/070174-08$04.00

We show in this paper that the energy gap experimentally observed by us in the low-frequency (quasi-ferromagnetic) branch of AFMR in YFO_3 in a spin-flip phase transition of second order, in a field directed along the **a** axis, exceeds considerably the magnetoelastic gap, and the "soft" mode in this transition is the relaxation one (soft relaxator). What is fundamental here is that this mode appears in the calculation only when dissipation processes are taken into account, and is due to the presence of at least two degrees of freedom which must be taken into account for this phase transition. One of them, usually invoked to describe orientational phase transitions, is connected with the rotation of the antiferromagnetism vector relative to the crystallographic axes. The other degree of freedom reflects the possibility of a change of the sublattice magnetic moments in the direction of the antiferromagnetism axis. The Landau-Lifshitz equations can therefore not be used to describe the antiferromagnetism dynamics for such phase transitions, and it is necessary to use the thermodynamic equations.[2,13]

Investigations of the low-frequency mode of AFMR in $YFeO_3$ near a spin-flip transition in a field directed along the **a** axis were carried out earlier. The measurements in Ref. 12 were made for a limited set of generator frequencies (at wavelengths 2, 4, 6, and 8 mm), and did not yield the true dependence of the AFMR frequency on the applied field. We note that the authors of Ref. 12 failed also to relax the AFMR frequency (to split the absorption lines) in the transition field at frequencies lower than 128 GHz. This, however, was attributed to inexact orientation of the crystal in the magnetic field. The temperature dependences of the gap in the AFMR spectrum of $YFeO_3$ in a zero external field were investigated in Refs. 14–16. The frequencies of the quasiferromagnetic modes were measured in Ref. 17 in magnetic fields up to 12 kOe. Thus, the experiments performed to date on AFMR in $YFeO_3$ were not complete, and this prompted the present investigation which led to hitherto unknown properties of magnets.

We have investigated the quasiferromagnetic AFMR mode in $YFeO_3$ at room temperature and at a large number of frequencies in the 60–400 GHz (λ = 5–0.75 mm) interval in stationary magnetic fields up to 130 kOe. Analysis of the experimental results revealed the form of the phase diagram at the observed spin flip, the thermodynamic variation of the system with change of the magnetic field, and the values of the energy gaps, of the thermodynamic-potential parameters, of the transport coefficients of the equations of motion, as well as of the ratio of the parallel and perpendicular susceptibilities. These are fundamental properties of antiferromagnets with weak ferromagnetism.

GROUND STATE AND PHASE DIAGRAMS FOR SPIN FLIP

To analyze the static and dynamic properties of $YFeO_3$ we start with the following thermodynamic potential

$$\Phi(\mathbf{M},\mathbf{L})=\tfrac{1}{2}B\mathbf{M}^2+\tfrac{1}{2}D(\mathbf{ML})^2+\tfrac{1}{2}D'\mathbf{M}^2\mathbf{L}^2+d_1M_xL_z-d_3M_zL_x-\mathbf{MH}+\tfrac{1}{2}a_1L_x^2+\tfrac{1}{2}a_2L_y^2+\tfrac{1}{2}a_3L_z^2+\tfrac{1}{4}a_{11}L_x^4+\tfrac{1}{2}a_{22}L_y^4+\tfrac{1}{4}a_{33}L_z^4+\tfrac{1}{2}a_{12}L_x^2L_y^2+\tfrac{1}{2}a_{13}L_x^2L_z^2+\tfrac{1}{2}a_{23}L_y^2L_z^2+\lambda(\mathbf{L}^2-L_0^2). \quad (3)$$

Here $\mathbf{M}=\mathbf{M}_1+\mathbf{M}_2$ and $\mathbf{l}=\mathbf{M}_1-\mathbf{M}_1$, where $\mathbf{M}_1$ and $\mathbf{M}_2$ are the sublattice magnetizations; B, D, and D' are the constants of the symmetric isotropic exchange interaction; d_1 and d_3 are the constants of the antisymmetric exchange interaction (the Dzyaloshinskiĭ-Moriya interaction), a_1 and a_{1j} are the constants of the anisotropic interactions; **H** is the external field, and λ is a Lagrange multiplier.

Let us discuss the assumptions made for the potential (3) above. First, the customarily employed additional assumption $\mathbf{M}_1^2=\mathbf{M}_2^2=$ const, which eliminates two degrees of freedom right away, were replaced by the condition $\mathbf{L}^2=$ const, which excludes only one degree of freedom. Second, we disregard the four-sublattice structure of orthoferrites,[18] confining ourselves to the two-sublattice approximation. As shown in Ref. 19, allowance for the presence of four sublattices leads to the appearance of two more (exchange) oscillation modes and influences little the relatively low-frequency AFMR modes considered here, which lead only to renormalization of anisotropy constants. Account is also taken in the expression for the thermodynamic potential of the fact that the inequality $\mathbf{M}^2/\mathbf{L}^2\ll 1$ is actually satisfied in orthoferrites in realistically attainable fields (on the order of hundreds of kOe), and therefore isotropic terms of order not higher than the second are retained in the expansion of the potential in terms of **M**. The expansion in terms of the components of the vector **L** was carried out only up to biquadratic terms. Since it is known from experiments on the magnetization of $YFeO_3$ (Ref. 19) that the constants d_1 and d_2 are equal to within several percent, we put $d_1=d_2=d$. In addition, we disregard in the present paper the interaction between the magnetic and the elastic subsystems. We shall estimate below the contribution of the magnetoelastic interaction to the AFMR frequencies.

Let us determine the ground state of the system. The equilibrium value of the vector **M** is obtained by minimizing the potential (3) with respect to M_x, M_y, and M_z:

$$\mathbf{M}_0=\chi_\perp(\mathbf{H}+\mathbf{H}_D)-(\chi_\perp-\chi_\parallel)(\mathbf{LH})\mathbf{L}/L_0^2, \quad (4)$$

$$\chi_\perp^{-1}=(B+D'L_0^2),\ \chi_\parallel^{-1}=\chi_\perp^{-1}+DL_0^2,\ \mathbf{H}_D=(-dL_z,\ 0,\ dL_x).$$

To find the equilibrium values of the vector **L** it is more convenient to transform to the angular coordinates

$$L_x=L_0\cos\theta\cos\varphi,\quad L_y=L_0\sin\theta,\quad L_z=-L\cos\theta\sin\varphi, \quad (5)$$
$$0\leqslant\theta\leqslant\pi/2,\ -\pi/2\leqslant\varphi\leqslant\pi/2.$$

It is easy to verify that in the absence of an external field there exists a solution $\theta=\varphi=0$ which agrees, in orthoferrites with nonmagnetic R-ions, with the actually observed state[20] (the L_xM_z state).

The analysis of the ground state and, next, the calculation of the frequencies in the presence of an external field, will be carried out for two cases, with the field directed along the **c** axis (z axis) or the **a** axis (x axis).

We introduce first the notation used hereafter:

$$H_E=\chi_\perp^{-1}L_0,\ H_D=dL_0,\ \eta=(\chi_\perp-\chi_\parallel)/\chi_\perp,$$
$$H_{ac}=L_0[a_3-a_1+(a_{13}-a_{11})L_0^2],$$
$$H_{ab}=L_0[a_2-a_1+(a_{12}-a_{11})L_0^2],\ H_{bc}=L_0[a_2-a_3+(a_{23}-a_{33})L_0^2],$$
$$H_{A2}=L_0^3(a_{11}+a_{33}-2a_{13}),\ H_{A2}'=L_0^3(a_{11}-a_{13}+a_{23}-a_{12}).$$

In a field directed along the **c** axis, the ground state of the vector **L** does not change; we do not obtain the range of the thermodynamic-potential constants in which this state is stable.

In a field directed along the **a** axis, the equilibrium values of the angle φ are determined from the equation

$$(\partial\Phi/\partial\varphi)_{M=M_0,\ \theta=0}$$
$$=\cos\varphi(H_EH_{ac}\sin\varphi+H_{A2}\sin^3\varphi-\eta H^2\sin\varphi-HH_D)=0. \quad (6)$$

It can be seen from (6) that in the case **H**||**a** there can exist a collinear phase

$$\cos\varphi=0, \quad \mathbf{LH}=0 \tag{7}$$

and a canted phase determined by the vanishing of the expression in the parentheses.

To construct the phase diagram, we consider the second-derivatives matrix

$$\{\alpha_{ij}'\}=\partial^2\Phi/\partial Y_i\partial Y_j; \quad Y_i, Y_j=M_x, M_y, M_z, \varphi, \theta. \tag{8}$$

Calculations have shown that in the case **H**||**c** the initial L_xM_z phase remains stable.

The most interesting situation arises in the case **H**||**a**. The matrix $\{\alpha_{ij}'\}$ is reduced here to a block-diagonal form (θ, M_y and M_x, M_z, and φ are separated). It is known[12,19-21] that in a magnetic field parallel to the **a** axis of the crystal the spin flip takes place in the **ac** plane; we consider therefore the stability with respect to the variables M_x, M_z, and φ. From the condition that the collinear phase ($\cos\varphi=0$) be stable to variations of the angle and to variation of the combination of the variables M_z and φ, we obtain equations for the fields in which the transition to the canted phase takes place:

$$H_t'=-H_D/2+[H_D^2/4+H_E(H_{ac}+H_{A2})]^{1/2}, \tag{9}$$

$$H_t=\eta^{-1}\{-H_D/2+[H_D^2/4+\eta H_E(H_{ac}+H_{A2})]^{1/2}\}. \tag{10}$$

As seen from a comparison of (9) and (10), allowance for the nonzero susceptibility $\chi_\parallel$ in the direction of the antiferromagnetism axis increases the transition field ($H_t/H_t'=1.1$ in $YFeO_3$ at $\chi_\parallel/\chi_\perp=0.3$); at $\chi_\parallel=0$ the conditions (9) and (10) are identical. Note that (10) can be obtained from the equation of state (6) by putting in the latter $\sin\varphi=1$.

Substitution of the equation of state in the condition for the stability of the canted phase changes the latter into

$$\cos^2\varphi(H_EH_{ac}-\eta H^2+3H_EH_{A2}\sin^2\varphi)\geqslant 0. \tag{11}$$

The principal task of the present paper is to construct the phase diagram for the investigated spin flip. It turned out that the phase diagram, which depends as usual on the coefficients of the Landau thermodynamic potential and is a complicated formation in multidimensional space, can be mapped uniquely, by a nonlinear transformation of the coordinates, on a two-dimensional plane pq, where

$$p=\frac{HH_D}{H_E|H_{A2}|}, \quad q=\frac{H_EH_{ac}-\eta H^2}{H_E|H_{A2}|} \tag{13}$$

are dimensionless parameters. In terms of these somewhat unusual coordinates the phase diagrams shown in Figs. 1 and 2 have a standard form (first- and second-order phase-transition lines, tricritical point, etc.). We point out specially that for a variable magnetic field and a constant temperature the thermodynamic plot on the given phase diagrams is no longer a straight line parallel, as usual, to one of the coordinate axes, but is a curve, some part of which is shown in Fig. 1 for the thermodynamic plot investigated by us (line MN, only the magnetic field changes).

In terms of the indicated variables, the stability conditions (11) and the equations of state (6) reduce to the form

$$\cos^2\varphi(q+3\,\mathrm{sign}\,H_{A2}\sin^2\varphi)\geqslant 0, \tag{13}$$

$$q\sin\varphi-p+\mathrm{sign}\,H_{A2}\sin^3\varphi=0, \tag{14}$$

$$\mathrm{sign}\,H_{A2}=H_{A2}'/|H_{A2}|.$$

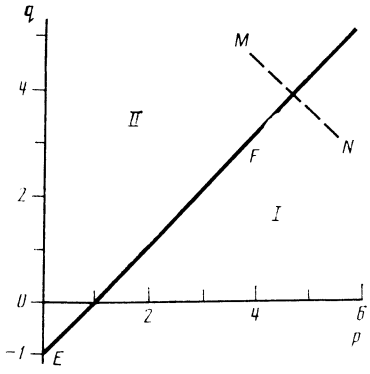

FIG. 1. Phase diagram in a field directed along the **a** axis for the case $H_{A2}>0$; $q=(H_EH_{ac}-\eta H^2)/H_E|H_{A2}|$; $p=HH_D/H_E|H_{A2}|$; I—stability region of the collinear ($\cos\varphi=0$) phase; II—stability region of the canted phase. The dashed line shows the thermodynamic path for $YFeO_3$ at $T=293$ K.

Since the topology of the phase diagram depends on sign H_{A2}, we consider hereafter separately the situations $H_{A2}>0$ (sign $H_{A2}=1$) and $H_{A2}<0$ (sign $H_{A2}=-1$). In the former case we find from (13) that the stability of the canted phase is lost only at $\sin\varphi=1$. The stability-loss line $p=q+1$ of the canted phase coincides in this case with the line of the onset of the collinear phase. This means that in our case the transition between the canted and collinear phases can be only of second order. The corresponding phase diagram is shown in Fig. 1.

The phase diagram for the case $H_{A2}<0$ is shown in Fig. 2. At $p\geqslant 2$ the stability-loss lines of the canted and collinear phases coincide and here, just as in the case H_{A2}, a second-order phase transition takes place. At $0\leqslant p\leqslant 2$ the stability regions of both phases overlap, and the transition between the canted and collinear phases should be of first order. We note once more that in the variables p and q the phase diagrams of the spin flip in a field **H**||**a** are the same for all orthorhombic crystals with magnetic configuration M_zL_x.

Reduction[19] of the experimental data on the magnetization of $YFeO_3$ has shown that H_{A2} is positive at 4.2 K and amounts in our notation to $\approx 0.1\,H_{ac}$. Consequently, if the field is exactly oriented along the **a** axis, the transition from the canted to the collinear phase should in this case certainly be of second order.

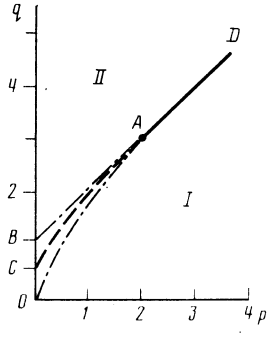

FIG. 2. Phase diagram in a field directed along the **a** axis for the case $H_{A2}<0$; BAD—stability-loss line of collinear phase; OAD—stability-loss line of the canted phase; CA—line of equal energies. The remaining notation is the same as in Fig. 1.

DETERMINATION OF THE AFMR FREQUENCIES

To find the antiferromagnetic-resonance frequencies we use first the hydrodynamic equations of motion without dissipation[2,22]:

$$\dot{\mathbf{M}}=\dot{\Delta\mathbf{M}}=\gamma_1[\mathbf{M}_0\mathbf{H}_M]+\gamma_2[\mathbf{L}_0\mathbf{H}_L],$$
$$\dot{\mathbf{L}}=\dot{\Delta\mathbf{L}}=\gamma_2[\mathbf{L}_0\mathbf{H}_M]+\gamma_3[\mathbf{M}_0\mathbf{H}_L]. \quad (15)$$

Here, $\mathbf{H}_M=\partial\Delta\Phi/\partial\Delta\mathbf{M}$; $\mathbf{H}_L=\partial\Delta\Phi/\partial\Delta\mathbf{L}$; $\Delta\Phi$ is the additional thermodynamic potential due to the deviation of the system from equilibrium:

$$\Delta\Phi=\tfrac{1}{2}\sum_{i,j}\alpha_{ij}\Delta X_i\Delta X_j, \quad (16)$$

$\hat{\alpha}=\{\alpha_{ij}\}$ is the matrix of the stability (of the second derivatives) with respect to the variables $\mathbf{X}=(M_x,M_y,M_z,L_x,L_y,L_z)$. Taking (16) into account, we can also express the equations (15) in the form

$$d\Delta\mathbf{X}/dt=\hat{\gamma}\hat{\alpha}\Delta\mathbf{X}, \quad (17)$$

where τ is an antisymmetric dynamic matrix.[22]

Note that the approximation $\mathbf{M}_1^2=\mathbf{M}_2^2=\text{const}$ corresponds to $\tau_1=\tau_2=\tau_3$ (the Landau-Lifshitz equations). The constraint $\mathbf{L}^2=\text{const}$ chosen by us corresponds to the condition[2)] $\gamma_3=0$.

We seek the solution of the system (17), as usual, in the form

$$\Delta\mathbf{X}=\Delta\mathbf{X}_0e^{i\omega t}. \quad (18)$$

Solving the secular equation of the system (17), we obtain two natural oscillation frequencies ω_1 and ω_2 corresponding to the quasiferromagnetic and quasiantiferromagnetic modes.

In a field directed along the **c** axis, the frequencies are given by the equations (here and elsewhere $\Delta\gamma=\gamma_1-\gamma_2$)

$$\omega_1^2=\gamma_2^2H_EH_{ac}+\frac{\chi_\perp}{\chi_\parallel}\Delta\gamma^2H_D^2+\left[\gamma_1^2+\left(2\frac{\chi_\perp}{\chi_\parallel}-1\right)\Delta\gamma^2\right]HH_D$$
$$+\left[\gamma_1^2+\left(\frac{\chi_\perp}{\chi_\parallel}-1\right)\Delta\gamma^2\right]H^2, \quad (19)$$
$$\omega_2^2=\gamma_2^2(H_EH_{ab}+H_D^2)+\gamma_2^2HH_D. \quad (20)$$

In a field directed along the **a** axis, the frequencies in the collinear phase ($H\geqslant H_t$) are given by

$$\omega_1^2=-\gamma_2^2H_E(H_{ac}+H_{A2})+\frac{\chi_\perp}{\chi_\parallel}\Delta\gamma^2H_D^2$$
$$+\left[\gamma_1^2+\left(2\frac{\chi_\perp}{\chi_\parallel}-1\right)\Delta\gamma^2\right]HH_D$$
$$+\left[\gamma_1^2+\left(\frac{\chi_\perp}{\chi_\parallel}-1\right)\Delta\gamma^2\right]H^2, \quad (21)$$
$$\omega_2^2=\gamma_2^2(H_EH_{ac}+H_D^2)+\gamma_2^2HH_D, \quad (22)$$

and in the canted phase ($H\leqslant H_t$), the expressions are unwieldy and are given here under the assumption[3)] $\gamma_1=\gamma_2=\gamma$:

$$\omega_{1,2}^2=\tfrac{1}{2}\gamma^2\{P+Q+R\mp[(P-Q+R)^2+4QR]^{1/2}\}, \quad (23)$$

where

$$P=H_E(H_{ab}+H'_{A2}\sin^2\varphi)+H_D^2-\eta H^2,$$
$$Q=H_E(H_{ac}+3H_{A2}\sin^2\varphi)\cos^2\varphi+H^2(\sin^2\varphi-\eta),$$
$$R=H^2(1+\eta)^2\cos^2\varphi. \quad (24)$$

Substitution of the threshold field H_t of the transition from the canted to the collinear phase in Eq. (21) leads to a nonzero frequency of the quasiferromagnetic mode at a second-order phase-transition point:

$$\omega_1^2|_{H=H_t}=\frac{\chi_\parallel}{\chi_\perp}\left[\gamma_2H_t+\Delta\gamma\frac{\chi_\perp}{\chi_\parallel}(H_t+H_D)\right]^2. \quad (25)$$

As already noted in the Introduction, the presence of a gap may mean that some oscillation modes were lost in the analysis of the secular equation of the system (17) because of the special form of the equations of motion (in the present case, because dissipation was not taken into account). We consider next, therefore, equations of motion containing terms that describe dissipative processes:

$$\dot{\Delta\mathbf{M}}=\gamma_1[\mathbf{M}_0\mathbf{H}_M]+\gamma_2[\mathbf{L}_0\mathbf{H}_L]+\alpha_1\mathbf{H}_M+\beta_1\mathbf{L}_0(\mathbf{L}_0\mathbf{H}_M),$$
$$\dot{\Delta\mathbf{L}}=\gamma_2[\mathbf{L}_0\mathbf{H}_M]+\gamma_3[\mathbf{M}_0\mathbf{H}_L]+\alpha_2\mathbf{H}_L+\beta_2\mathbf{L}_0(\mathbf{L}_0\mathbf{H}_L). \quad (26)$$

Here α_1, α_2, β_1 and β_2 are phenomenological relaxation parameters. Equations (25), just as (15), are written in the exchange approximation.

We consider the case of the collinear phase at $H\gg H_t$. This simplifies substantially the calculations and yields exact equations for the low-frequency oscillation modes of interest to us:

$$(-i\omega+\varepsilon')\Delta L_x+c_1\Delta M_y+\varepsilon''\Delta M_z=0,$$
$$c_2\Delta L_x+(-i\omega+\varepsilon_\perp)\Delta M_y+c_3\Delta M_z=0,$$
$$\varepsilon'''\Delta L_x+c_4\Delta M_y+(-i\omega+\varepsilon_\parallel)\Delta M_z=0. \quad (27)$$

Here

$$c_1=\gamma_2H_E,\quad c_2=\Delta\gamma\frac{H+H_D}{H_E}K+H_{ac}+H_{A2},$$
$$K=\frac{\chi_\perp}{\chi_\parallel}(H+H_D)-H,$$
$$c_3=-\gamma_2H+\Delta\gamma\frac{\chi_\perp}{\chi_\parallel}(H+H_D),\quad c_4=\gamma_1(H+H_D),$$
$$\varepsilon_\perp=\alpha_1\chi_\perp^{-1},\ \varepsilon_\parallel=(\alpha_1+\beta_1L_0^2)\chi_\parallel^{-1},$$
$$\varepsilon'=\frac{\alpha_2}{L_0}\left(\frac{H+H_D}{H_E}K+H_{ac}+H_{A2}\right),$$
$$\varepsilon''=-\frac{\alpha_2K}{L_0},\quad \varepsilon'''=-\frac{\alpha_1+\beta_1L_0^2}{L_0}K.$$

Since the inequalities $H_E\gg H_t$, $H_D\gg H_{ac}$, H_{A2} are satisfied in the considered orthoferrites, we have the following relations for the parameters ε connected with the dissipation:

$$\varepsilon_\perp,\ \varepsilon_\parallel\gg\varepsilon',\ \varepsilon'',\ \varepsilon'''. \quad (28)$$

With (28) taken into account, the secular equation of the system (27) is of the form

$$i\omega^3-A\omega^2-i\omega B+C=0, \quad (29)$$

where

$$A=\varepsilon_\perp+\varepsilon_\parallel,\quad B=\omega_1^2,$$
$$C=\varepsilon_\parallel\omega_3^2,\quad \omega_3^2=\gamma_2^2[\eta H^2+HH_D-H_E(H_{ac}+H_{A2})],$$

ω_1 is the frequency of the quasiferromagnetic mode without allowance for dissipation and is given by Eq. (21). We see that when dissipation is taken into account the secular equation becomes cubic. Solving this equation (assuming low dissipation),[4)] we obtain the following three complex natural frequencies of the oscillations:

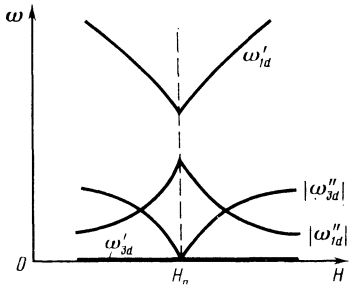

FIG. 3. Approximate plots of the real and imaginary parts of the AFMR quasiferromagnetic mode ($\omega_{1d}=\omega'_{1d}+i\omega''_{1d}$) and relaxation mode ($\omega_{3d}=i\omega''_{3d}$) near a second-order phase transition.

$$\omega_{1d,\,2d}=\pm\omega_1-i\varepsilon_a. \tag{30}$$

$$\omega_{3d}=-i\varepsilon_{\parallel}\omega_3^2/\omega_1^2, \tag{31}$$

the first two of which are the frequencies of the quasiferromagnetic mode with damping

$$\varepsilon_a=\frac{1}{2}\varepsilon_{\perp}+\frac{1}{2}\varepsilon_{\parallel}\frac{\chi_{\parallel}}{\chi_{\perp}}\frac{\gamma_2^2H^2}{\omega_1^2}, \tag{32}$$

and the third is the frequency of the relaxation mode. Qualitative plots of the real and imaginary parts of ω_{1d} and ω_{3d} are shown in Fig. 3. It can be seen that it is precisely the relaxation mode which has a singularity in the phase transition, viz., besides the real part, which is identically zero, the imaginary part of the complex frequency is also zero. We emphasize once more that without allowance for the susceptibility in the direction of the antiferromagnetism axis and for the dissipation, the relaxation mode simply drops out. We note also that experimental observation of a gap in the spectrum of the quasiferromagnetic mode at a second-order phase-transition point is an indirect indication of the existence of a relaxation mode.

EXPERIMENTAL PROCEDURE AND REDUCTION OF RESULTS

We measured in the experiment the positions of the absorption lines, due to the electromagnetic radiation incident on the sample, as functions of the applied magnetic field at $T=293$ K. The measurements were made with the setup described in Ref. 23. The radiation (60–400 GHz, $\lambda=5$–0.75 mm) was produced by backward-wave oscillators. The wavelength was measured with a Fabry-Perot interferometer[24] with reticular mirrors, at an accuracy not worse than 0.5%. The radiation was transmitted through a multimode light waveguide to a receiver based on *n*-InSb and cooled to 4.2 K. The magnetic field was produced by the "Solenoid" apparatus of the strong-magnetic-field department of our institute.[25] The field was calibrated to within 1% from the positions of the EPR lines in DPPH mounted on the sample. The $YFeO_3$ samples were obtained by crucibleless zone melting with radiative heating[26] and were plates with transverse dimensions 3×6 mm, oriented perpendicular to the **a** or **c** axis of the crystal. We investigated only three samples, of which two were cut from one bulky single crystal and were oriented by x-ray diffraction accurate to $\pm1°$ in the direction of the **a** or **c** axis of the crystal. The sample thicknesses were 0.5 and 1 mm, respectively. The third sample, obtained from a different melt, was perpendicular to the **c** axis and 0.1 mm thick. All the samples were annealed in oxygen in accordance with the following schedule: 2 h heating to 1300 °C, 4 h kept at this temperature, and 2 h cooling. The AFMR line width of the annealed crystals was 0.5–1 kOe, as against 2–5 kOe for those not annealed. According to calculations made in Refs. 27 and 12, the minimum value of the AFMR frequency in a field applied to along the **a** axis is extremely sensitive to even a small deflection from the axis in the **ac** plane and depends little on the deflection of the field in the **ab** plane.

In view of the fundamental importance of the results (observation of an appreciable energy gap in the spin-wave spectrum at a second-order phase transition point), let us dwell in greater detail on the procedure used to orient the sample. Precise orientation of the crystal in the magnetic field in the direction of the **a** axis was implemented with a rotating stage on which the sample was mounted, and adjusting screws that permitted to the waveguide to be tilted in two planes, and was effected in two stages. During the first stage, the crystal was positioned in such a way that the splitting of the AFMR lines for $H<H_t$ and $H>H_t$ was a maximum. The frequency was then lowered and the orientation was improved; this was repeated down to frequencies at which the splitting of the resonance lines was still noticeable. In the second stage the external magnetic field was fixed at a value at which the change of the resonance-line intensity was a maximum, and the final setting was adjusted by coordinated rotation of the adjustment screws. (The second adjustment stage is illustrated in Fig. 4, which shows examples of the AFMR lines obtained at different frequencies at the best achieved orientation of the sample.) In the presence of a practically continuous frequency spectrum, this procedure made possible a highly accurate ($\pm3'$) orientation of the sample in the magnetic field.

The measurement results (which were the same within the limits of experimental error for all three samples), in a field applied in the direction of the axis **a** or **c**, are shown in Fig. 5. The inset shows in enlarged scale the dependence of the squared AFMR frequency on the field close to the com-

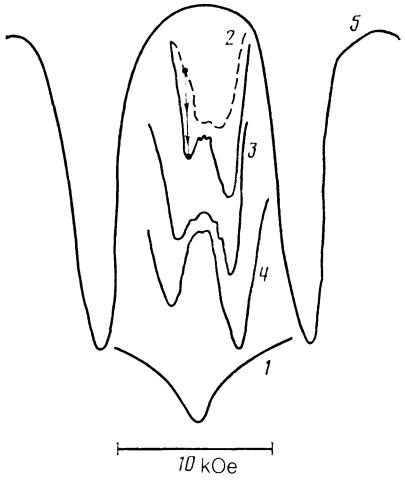

FIG. 4. Typical plots of AFMR lines of $YFeO_3$ for $T=293$ K and different frequencies: 1—75 GHz, 2—127 GHz, 3—130 GHz, 4—131.6 GHz, 5—168.5 GHz. The arrow shows the change of the signal intensity on improvement of the orientation in a fixed magnetic field.

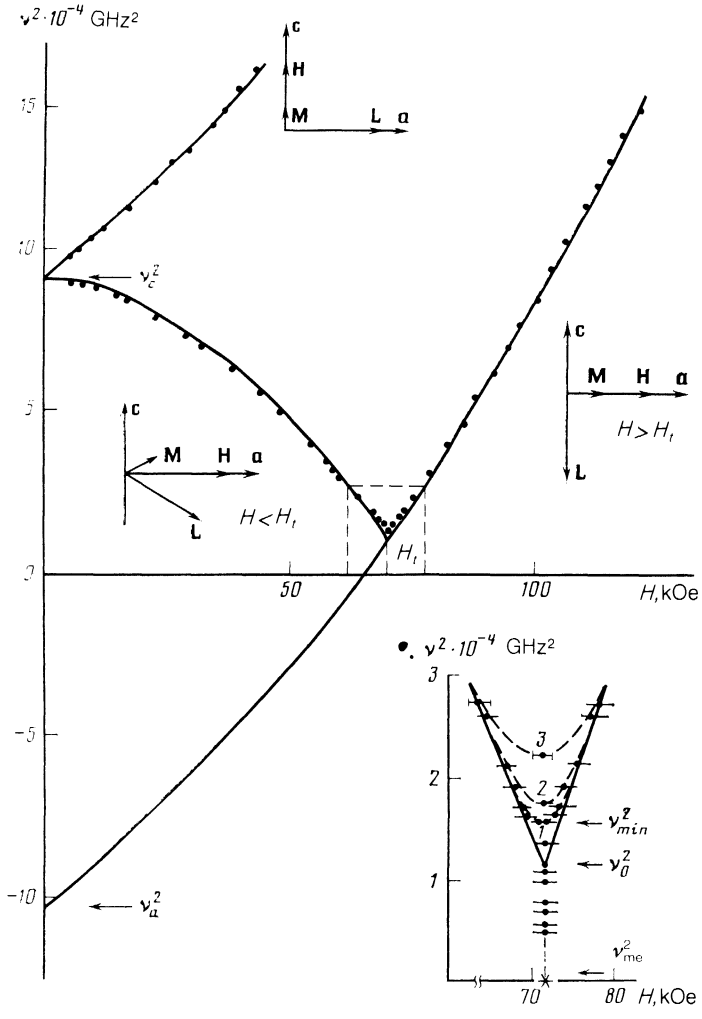

FIG. 5. Plots of the squared frequency of the quasiferromagnetic AFMR mode of $YFeO_3$ in a field directed along the axis **a** or **c** at $T = 293$ K. Points—experimental data, solid curve—calculated. The inset shows in enlarged scale the $\nu^2(H)$ dependence near the completion of the spin-flip transition at small deviation of the sample position from exact orientation: 1—exact orientation, 2—5′, 3—30′; $\nu_c = 302$ GHz $\pm$ 2%, $\nu_a = -326$ GHz $\pm$ 3%, $\nu_{min} = 126$ GHz $\pm$ 2%, $\nu_0 = 107$ GHz $\pm$ 2%, $\nu_{me} = 20$ GHz, $H_t = 71.5 \pm 1$ kOe.

pletion of the spin-flip transition. Curve 1 of the figure corresponds to the maximum attained accuracy of the sample orientation. Curves 2 and 3 were obtained with the magnetic field deflected 5′ and 30′ respectively from the optimum position in the **ac** plane. The minimum energy gap obtained in the experiment was 126 GHz $\pm$ 2%. It should be noted that at exact field orientation there was observed, near the completion of the spin-flip transition, all the way to 60 GHz, gradually fading unsplit absorption lines, just as in Ref. 12, which we attribute to "tails" of the AFMR lines. Observation of these lines made it possible to determine the transition field $H_t = 71.5$ kOe accurate to $\pm$ 0.5 kOe.

The measurement results were reduced as follows. The field dependences of the AFMR frequencies in a field applied along the **c** axis, and also in a field along the **a** axis at $H > H_t$, were approximate in accordance with Eqs. (19) and (21) by polynomials of the form

$$\omega_{c,a}^2/\gamma_0^2 = \alpha_{c,a} + \beta_{c,a} H + \tau H^2, \tag{33}$$

where τ_0 is the gyromagnetic ratio. We first calculated by least squares the experimental values of α_c, α_a and β_c, β_a as functions of τ in the range $0.8 \leqslant \tau \leqslant 1.2$; we determined at the same time the mean squared deviation $\delta_{c,a}(\tau)$ of the calculated curve from the experimental one. It was found that δ_a depends little on τ; δ_c shows only a weak minimum near $\tau = 1$. The calculated values of α_c and α_a remain within the limits of the experimental accuracy as τ is varied from 0.8 to 1.2, and turn out to equal (at $\tau = 1$)

$$\alpha_a = -(137 \pm 3)\,10^2 \text{ kOe}^2, \quad \alpha_c = (116 \pm 0.5)\,10^2 \text{ kOe}^2.$$

The same values of α_c was obtained by reducing the experimental results with the aid of Eq. (33) in the case $\mathbf{H} \| \mathbf{a}$ in fields up to 15 kOe.

To determine the values of β_a and β_c we used the fact, which follows from (19) and (21), that they should satisfy the following relations:

$$\beta_a = \beta_c = \beta = \frac{1}{\gamma_0^2}\left[\gamma_1^2 + \left(2\frac{\chi_\perp}{\chi_\parallel} - 1\right)\Delta\gamma^2\right] H_D,$$

with

$$\tau = \frac{1}{\gamma_0}\left[\gamma_1^2 + \left(\frac{\chi_\perp}{\chi_\parallel} - 1\right)\Delta\gamma^2\right].$$

The values of β_a and β_c coincide for the calculated $\beta_a(\tau)$ and $\beta_c(\tau)$ dependences at a single points with coordinates $\tau = 1 \pm 0.01$ and $\beta = (140 \pm 2)$ kOe. From the experimentally obtained value for $\tau = 1$, and from the fact that for an ion in the S state, such as Fe^{+3}, we should have $\Delta\gamma/\gamma \ll 1$, it was concluded that this compound we have, accurate to about one percent,

$$\gamma_1 = \gamma_2 = \gamma_0. \tag{34}$$

The condition (34) makes it possible to simplify Eqs. (19) and (21) and to determine the energy gaps and the Dzyaloshinskiĭ fields:

$$H_E H_{ac} = (116 \pm 0.5)\, 10^2\ \text{kOe}^2,$$

$$H_E H_{A2} = (21 \pm 3)\, 10^2\ \text{kOe}^2,\quad H_D = (140 \pm 2)\ \text{kOe}.$$

The quantity $H_E H_{ac}$ agrees well with the data of Refs. 15 and 16 and differs somewhat from those of Ref. 14. The field H_D agrees with the value obtained from a static[20] experiment. The value of H_{A2} at $T = 293$ K, just as at $T = 4.2$ K (Ref. 19), turned out to be positive. This circumstance, as well as the fact no hysteresis phenomena whatever were observed in the experiment near the completion of the spin-flip, indicates that the phase transition in this case is of second order.

Extrapolation of the $\nu^2(H)$ dependence from the region of strong magnetic fields to the spin-flip-transition field (point A in Fig. 5) yields for the gap in the transition field a value $\nu_0 = 107$ GHz $\pm$ 2%, which is stable to field disorien tation up to 2° relative to the crystallographic axes in any direction, if the data are reduced using the experimental points from the region $H \geqslant 1.1 H_t$. As seen from Eq. (25), from the size of the gap in the transition field we can get the ratio $\chi_\parallel / \chi_\perp$ of the longitudinal and transverse antiferromagnetic susceptibilities. It is necessary here to subtract from the value of the gap the contribution due to the magnetoelastic interaction:

$$\nu_{me} = \frac{\gamma_0^2}{(2\pi)^2} H_E H_{me} = \frac{1}{2} \frac{\gamma_0^2}{(2\pi)^2} \frac{|E_a| \lambda_{aa}^2}{\chi_\perp}; \qquad (35)$$

here E_0 is the elastic modulus in the direction of the **a** axis, and λ_{aa} is the magnetostriction in the direction of the **a** axis in a field applied along the **a** axis.

To estimate this contribution we used the data of Refs. 19 and 20, viz., $\chi_\perp \approx 5 \cdot 10^{-5}$ at $YFeO_3$ density $\rho \approx 5$ g/cm^3, $\lambda_{aa} = -1.5 \cdot 10^{-5}$, and $E_a = -2 \cdot 10^{12}$ erg/cm^3. We obtained for the magnetoelastic gap a value not higher[5] than 20 GHz, i.e., much lower than observed in experiment. This made it possible to determine from a dynamic experiment the ratio $\chi_\parallel / \chi_\perp = 0.3 \pm 0.03$ of the parallel and perpendicular susceptibilities. This ratio agrees with the value obtained in the molecular-field theory.

Using the values of $H_E H_{ac}$, $H_E H_{A2}$, H_D and $\chi_\parallel / \chi_\perp$ determined above, we used Eq. (23) to plot the $\nu^2(H)$ dependence in the canted phase at $0 \leqslant H \leqslant H_t$; as seen from Fig. 4, the theoretical curve agrees, to within the plotting accuracy, with the experimental points.[6]

CONCLUSIONS

We conclude by formulating briefly our main results.

1. Assuming $\mathbf{L}^2 = \text{const}$, phase diagrams were plotted for a rhombic antiferromagnet with weak ferromagnetism in a field directed along the **a** axis (which coincides with the initial direction of the antiferromagnetism vector); it was shown that the topology of the phase diagrams depends on the sign of the combination of the biquadratic anisotropy constants. An equation was obtained for the spin-flip-transition field at nonzero temperature; this equation depends on the susceptibility in the direction of the antiferromagnetism axis.

2. Assuming $\mathbf{L}^2 = \text{const}$, a theory of antiferromagnetic resonance was developed for a rhombic antiferromagnet with weak ferromagnetism for the case of spin flip in a field directed along the **a** axis, with dissipation processes taken into account. It was shown that besides the known oscillation modes of the antiferromagnetic resonance there should exist also a relaxation mode of the oscillations, which is "soft" for the spin-flip transition. The frequency of the quasiferromagnetic mode in a second-order phase transition should differ from zero.

3. An appreciable energy gap of nonmagnetoelastic origin was experimentally observed in the spectrum of the low-frequency quasiferromagnetic mode for a second-order spin-flip transition in yttrium orthoferrite $YFeO_3$, in an external field directed along the **a** axis.

4. The low-frequency AFMR mode in $YFeO_3$ was experimentally investigated at frequencies 60–400 GHz and at $T = 293$ K, in magnetic fields up to 130 kOe directed along the axes **c** and **a**. The values of the energy gaps, transport coefficients, Dzyaloshinskiĭ field, and the ratio of the longitudinal and transverse susceptibilities were determined.

[1)] However, the gap observed in this substance could be due also to inaccurate orientation. This was pointed out, in particular, by the authors of Ref. 12.

[2)] This condition can be easily obtained by taking the scalar product of the last equation of (15) and $\mathbf{L}$: $\frac{1}{2}\partial \mathbf{L}^2/\partial t = -\gamma_3 \mathbf{H}_L [\mathbf{M}_0 \times \mathbf{L}_0]$, from which it can be seen that, since $\mathbf{L}_0$ is not collinear with $\mathbf{M}_0$, it follows from the constancy of $\mathbf{L}^2$ that $\gamma_3 = 0$.

[3)] The equations obtained by us for the frequencies in the canted phase differ from those of Ref. 12 even in the case $\eta = 1$.

[4)] This assumption, which takes the form $\omega_1 \gg \varepsilon_\perp, \varepsilon_\parallel$ is valid in the entire range of fields, since the AFMR spectrum of $YFeO_3$ has a gap.

[5)] The estimate obtained by us for the magnetoelastic gap agrees well with the experimental value 15 GHz (Ref. 18) observed in the orthoferrite $ErFeO_3$ in a second-order phase transition at low temperatures.

[6)] The value of $H_E H_{ab}$ needed for the calculations was taken from Ref. 16. Calculation has shown that variation of the unknown parameter $H_E H'_{A2}$ in Eq. (35), in a range $\pm 0.3 H_E H_{ab}$, necessitates insignificant (less than 1%) corrections for $\nu^2(H)$.

[1] E. M. Lifshitz and L. P. Pitaevskii, *Statistical Physics*, Part 2, Pergamon, 1980 (p. 367 of Russ. Orig.).
[2] Yu. M. Gufan, Zh. Eksp. Teor. Fiz. **60**, 1537 (1971) [Sov. Phys. JETP **33**, 831 (1972)]. VNIIFTRI Preprint No. 42, 1970.
[3] A. M. Rodichev, Zh. Eksp. Teor. Fiz. **48**, 860 (1965) [Sov. Phys. JETP **21**, 574 (1966)].
[4] I. E. Dzyaloshinskiĭ and B. G. Kukharenko, *ibid.* **70**, 2360 (1976) [**43**, 1232 (1976)].
[5] D. V. Volkov, A. A. Zheltukhin, and Yu. P. Bliokh, Fiz. Tverd. Tela (Leningrad) **13**, 1668 (1971) [Sov. Phys. Solid State **13**, 1396 (1972)].
[6] D. V. Volkov and A. A. Zheltukhin, Zh. Eksp. Teor. Fiz. **78**, 1867 (1980) [Sov. Phys. JETP **51**, 937 (1980)].
[7] P. W. Anderson, Phys. Rev. **112**, 1900 (1959).
[8] W. Cochran, Adv. Phys. **9**, 385 (1960); **10**, 401 (1961).
[9] V. L. Ginzburg, Usp. Fiz. Nauk **77**, 621 (1962) Sov. Phys. Usp. **5**, 649 (1963)].
[10] Yu. M. Gufan and E. S. Larin, Fiz. Tverd. Tela (Leningrad) **20**, 1725 (1978) [Sov. Phys. Solid State **20**, 998 (1978)].
[11] V. A. Sanina, E. I. Golovenchits, T. A. Fomina, and A. G. Gurevich, Phys. Lett. **33A**, 291 (1970).
[12] V. I. Ozhogin, V. G. Shapiro, K. G. Gurtovoĭ, E. A. Galst'yan, and A. Ya. Chervonkis, Zh. Eksp. Teor. Fiz. **62**, 2221 (1972) [Sov. Phys. JETP **35**, 1162 (1972)].
[13] E. G. Rudashevskiĭ, Abstracts, 16th All-Union Conf. on the Physics of Magnetic Phenomena, Tula, 198, p. 150.
[14] L. V. Velikov, E. A. Vitvinin, G. E. Ivannikova *et al.*, Fiz. Tverd. Tela (Leningrad) **22**, 3612 (1980) [Sov. Phys. Solid State **22**, (1980)].
[15] K. N. Kocharyan, R. M. Martirosyan, V. G. Prpryan, and E. L. Sarkisyan, Zh. Eksp. Teor. Fiz. **86**, 639 (1984) [Sov. Phys. JETP **59**, 373 (1984)].
[16] A. L. Volkov, Yu. G. Goncharov, G. V. Kozlov *et al.*, Pis'ma Zh. Eksp. Teor. Fiz. **39**, 140 (1984) [JETP Lett. **39**, 166 (1984)].
[17] A. M. Balbashov, T. S. Mandel'shtam, S. I. Nikitin, and A. S. Prokhorov, Kratk. Soobshch. Fiz. (FIAN) No. 2, 35 (1985).

[18]G. F. Herrman, Phys. Rev. **133**, 2334 (1964).
[19]F. S. Jacobs, H. F. Burne, and L. M. Levinson, J. Appl. Phys. **42**, 1631 (1971).
[20]K. P. Belov, A. K. Zvezdin, A. M. Kadomtseva, and R. Z. Levitin, Orientational Transitions in Rare-Earth Magnets [in Russian], Nauka, 1979.
[21]A. M. Balbashov, A. G. Berezin, Yu. M. Gufan *et al.*, Pis'ma Zh. Eksp. Teor. Fiz. **41**, 391 (1985) [JETP Lett. **41**, 479 (1985)].
[22]Yu. M. Gufan, A. S. Prokhorov, and E. G. Rudashevskiĭ, FIAN Preprint No. 61, 1979.
[23]E. G. Rudashevsky, A. S. Prochorov, and L. B. Velikov, IEEE Trans. **MMT-22**, 1064 (1974).
[24]E. A. Vinogradov, E. M. Dianov, and N. A. Irisova, Pis'ma Zh. Eksp. Teor. Fiz. **2**, 323 (1965) [JETP Lett. **2**, 205 (1965)].
[25]V. G. Veselago, L. P. Maksimov, and A. M. Prokhorov, Prib. Tekh. Eksp. No. 4, 192 (1968).
[26]A. M. Balbashov, A. Ya. Chervonkis, A. V. Antonov, and V. E. Bakteuzov, Izv. AN SSSR, ser. fiz. **35**, 1241 (1971).
[27]F. B. Hagedorn and E. M. Gyorgy, Phys. Rev. **174**, 540 (1968).
[28]N. K. Dan'shin, N. M. Kovtun, and M. A. Sdvizhkov, Fiz. Nizk Temp. **8**, 285 (1982) [Sov. J. Low Temp. Phys. **8**, 143 (1982)].

Translated by J. G. Adashko